CHEMISTRY
A European Journal

A Journal of
ChemPubSoc Europe

Accepted Article

Title: Alkyl Triarylstannanecarbodithioates: Synthesis, Crystal Structures and Efficiency in RAFT Polymerization

Authors: Ihor Kulai, Nathalie Saffon-Merceron, Zoia Voitenko, Stéphane Mazières, and Mathias Albin Destarac

To be cited as: *Chem. Eur. J.* 10.1002/chem.201703412

Link to VoR: http://dx.doi.org/10.1002/chem.201703412

Supported by
ACES

WILEY-VCH

10.1002/chem.201703412

WILEY-VCH

FULL PAPER

Alkyl Triarylstannanecarbodithioates: Synthesis, Crystal Structures and Efficiency in RAFT Polymerization

Ihor Kulai,[a] Nathalie Saffon-Merceron,[b] Zoia Voitenko,[c] Stéphane Mazières,*[a] Mathias Destarac*[a]

Abstract: Eight alkyl triarylstannanecarbodithioates were synthesised starting from the corresponding triarylstannyl chlorides. They were fully characterised by IR and ^{1}H, ^{13}C and ^{119}Sn NMR spectroscopies, and by mass spectrometry. Their solid-state structures and geometric parameters were determined and compared to those of other classes of thiocarbonylthio compounds. These new organotin derivatives are efficient reversible chain transfer agents for reversible addition-fragmentation chain transfer (RAFT) polymerization of styrene (St) and *n*-butyl acrylate (BA), with controlled number-average molecular weights (M_n) and narrow dispersities ($Đ$ < 1.3). In some cases, a loss of control of the polymerization was evidenced and supported by the observation of side products by ^{119}Sn NMR. This phenomenon was attributed to the thermal instability of the Sn-RAFT terminal group.

Introduction

Reversible Addition-Fragmentation chain Transfer (RAFT) polymerization[1] has been greatly improved since its invention in the mid-1990s.[2–5] Nowadays, it is one of the most versatile reversible deactivation radical polymerization (RDRP) techniques as it tolerates a diverse range of functional groups and reaction process conditions. RAFT technology allows low dispersity (co)polymers with controlled molecular weight to be obtained from a wide range of vinyl monomers through the use of different classes of RAFT agents of general formula Z(C=S)SR.[6]

The RAFT polymerization process can be summarized as an insertion of monomer units along the C-S bond of the RAFT agent as depicted in Scheme 1. Each molecule of RAFT agent gives rise to a polymer chain that possesses both *α*- and *ω*- chain ends derived from the initial agent. As a result, the obtained polymer is a RAFT agent itself and can be used for block copolymerization with other monomers[7] or post-polymerization chain-end transformations such as hetero-Diels-Alder coupling[8] or transformation into a thiol.[9–11] This latter process gives access to further coupling reactions, such as the thiol-ene click reaction.[12] The chain end can also be removed by radical-induced oxidation, reduction, or nucleophilic substitution reactions, as well as high temperature thermolysis, to prepare colorless, odorless and stable polymers.[9,13–15]

RAFT agents are categorized according to the structure of their Z group, including commonly used dithioesters, xanthates, trithiocarbonates, and dithiocarbamates.[6,16] Each of these classes is suited to a specific, and often limited, class of monomers. However, there are some examples of “uncommon” RAFT agents based on such heteroelements as fluorine,[17] phosphorus,[18–20] selenium[21–23] or silicon.[24] These elements bring characteristic properties which allow further tuning of the RAFT agents’ reactivities, and expand the field of their application, for example in the use of NMR techniques to monitor the polymerization process.[19–21,24,25] This addresses the limitations of ^{1}H or ^{13}C NMR for the analysis of polymers due to overlapping signals and low signal intensities.[26] Heteronuclear NMR with ^{19}F, ^{31}P, ^{77}Se or ^{119}Sn nuclei provide a separate NMR channel for the quantification of RAFT agent transformations. This approach can be used to study the RAFT agent consumption, its stability, the stability of the polymer *ω*-chain end, as well as to monitor post-polymerization transformations. Despite the 100% natural abundance of ^{19}F and high NMR sensitivity, ^{19}F NMR monitoring of RAFT processes has only been reported in one study.[27] Our team has used ^{31}P NMR and ^{119}Sn NMR to study the reactivity of RAFT agent, the nature of the chain end and the efficiency of block copolymerization with organophosphorus[19,20] and organotin[25] RAFT agents.

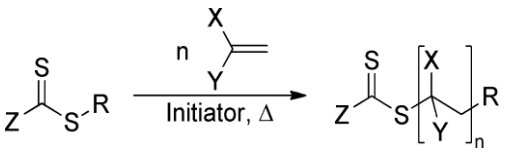

Scheme 1. Simplified representation of RAFT polymerization.

There is a rich literature on the radical chemistry of organotin reagents, and the first synthesis of a stannanecarbodithioate was reported in 1980.[28] Originally, they were studied as chelate ligands for transition metal complexes[29] and there are only a few reports on the preparation and properties of stannanedithiocarbonates.[29–38] In a recent communication, we reported the first use of triphenylstannanecarbodithioates in RAFT polymerization,[25] and studied their chain transfer activity using ^{119}Sn NMR. This technique also revealed the presence of side reactions at the *ω*-chain end.

In this study, we report the synthesis, characterization and crystal structures of a series of triarylstannanecarbodithioates (Scheme 2), and evaluate their efficiency in RAFT polymerization with simultaneous ^{1}H, ^{19}F and ^{119}Sn NMR monitoring.

[a] Dr. I. Kulai, Dr. S. Mazières, Prof. Dr. M. Destarac
Laboratoire des IMRCP, Université Paul Sabatier, CNRS UMR 5623
118 route de Narbonne 31062 Toulouse Cedex 9, France
E-mail: destarac@chimie.ups-tlse.fr, mazieres@chimie.ups-tlse.fr
[b] Dr. N. Saffon-Merceron
Institut de Chimie de Toulouse, CNRS FR 2599, Université Paul Sabatier
118 route de Narbonne 31062 Toulouse Cedex 9, France
[c] Prof. Dr.Sci. Z. Voitenko
Department of Chemistry, Taras Shevchenko National University of Kyiv
12, Lva Tolstoho Street, 01033, Kyiv, Ukraine

Supporting information for this article is given via a link at the end of the document.

10.1002/chem.201703412

Results and Discussion

The efficiency of RAFT agents is determined by the structure of their R and Z groups. For the current study, two triarylstannyl groups, triphenylstannyl (RAFT agents **1**-**6**, Scheme 2) and tri-*p*-tolylstannyl (RAFT agents **7** and **8**), were synthesized from the corresponding commercially available triarylstannyl chlorides. In addition to the original benzyl (RAFT agents **1** and **7**) and 1-phenylethyl R groups (RAFT agents **2** and **8**), we studied the effect of substituting a strongly electron-withdrawing nitro group (RAFT agent **3**) or a weakly electron-withdrawing fluorine (RAFT agent **4**) in the *para* position of the benzyl group. The fluorine substituent enables the use of ^{19}F NMR to monitor the transformations of RAFT agent **4** in the early stages of polymerization. Finally, the widely used cyanomethyl and 1-(methoxycarbonyl)ethyl R groups were selected (RAFT agents **5** and **6**).

Synthesis and characterization

Triarylstannanecarbodithioates **1**-**8** were prepared according to a slightly modified literature method (Scheme 2).[30,35,38] Originally, lithium metal was used to reduce the starting triarylstannyl chlorides to triarylstannyl anions. However, due to the negligible solubility of alkaline metals in THF, reaction takes place only on the lithium surface and overall conversion of the starting material lasts up to 72 hours even at elevated temperatures. The final products are frequently contaminated by hexaaryldistannanes. To avoid these drawbacks, sodium naphthalenide[39] was used as a reducing reagent. Due to its solubility in THF and extremely high reactivity, nearly quantitative reduction of triarylstannyl chlorides takes place in a few minutes in a highly exothermic reaction.

Subsequent treatment of the triarylstannyl anions with an excess of carbon disulfide leads to the formation of triarylstannanecarbodithioate salts that are detected immediately by the appearance of a characteristic red color. These salts are stable and can be isolated. However, they were used directly in solution without further purification. After alkylation and work up, the title triarylstannanecarbodithioates were isolated as pink or violet solids. All synthesized compounds are soluble in organic solvents such as THF, toluene, dichloromethane and 1,4-dioxane. They are not air-sensitive in the solid state or in solution, which is an advantage for storage and handling. However, compounds **5** and **6** have poor thermal stability at room temperature that prevents their use in free-radical polymerization.

As compound **5** is unstable even at -20°C, the only adequate proofs of its structure are low temperature X-ray diffraction and NMR spectroscopy analyses (Figures S14 to S16, and Table S1). Satisfactory spectroscopic and analytical data were collected for all other compounds of the study. Chemical ionization high resolution mass spectrometry (CI-HRMS/CH_4) of RAFT agents **1**-**4** and **6**-**8** revealed protonated molecular ion $[M+H]^+$ peaks with m/z that match the theoretical values. The ^{1}H NMR spectra (Figures S1, S4, S7, S10, S14, S17, S20 and S23) contain characteristic deshielded signals of the CH and CH_2 groups connected to sulfur with chemical shifts in the range from δ = 5.85 to 4.18 ppm. Their multiplicities confirm coupling of these protons with tin ($^4J_{Sn,H}$ = 2.3–7.3 Hz).

The ^{13}C NMR spectra (Figures S2, S5, S8, S11, S15, S18, S21 and S24) exhibit unusual resonances for the carbon atom of the CS_2 group in extremely weak field. Literature data on the ^{13}C NMR spectra of selected RAFT agents with benzyl or 1-phenylethyl R-group and variation of Z-groups (Figure S26) allowed the chemical shifts to be classified according to the central atom of the Z-group (Figure 1).[17,18,20,40–48] They range from 195.5 ppm for dithiocarbamates[42] to 242.6 ppm for phosphorylmethanedithioates,[20] whereas the chemical shifts of triarylstannanecarbodithioates range from 262.6 ppm to 266.3 ppm.

These chemical shifts are connected to the electrophilic character of the thiocarbonyl carbon, and are explained by the covalent radius of the central atom of the Z-group associated with the electronic effects it produces. In the cases of xanthates and dithiocarbamates, *π*-donation by the oxygen or nitrogen atoms explains most of the increase of electron density of the thiocarbonyl carbon and the resulting strong shielding of the chemical shifts, while with carbon, sulphur and phosphorus in the Z-group, the electron density decreases. For the electropositive tin, the electron donating effect is reduced by the size of the tin atom and the comparatively long Sn-C bond (Table 1).

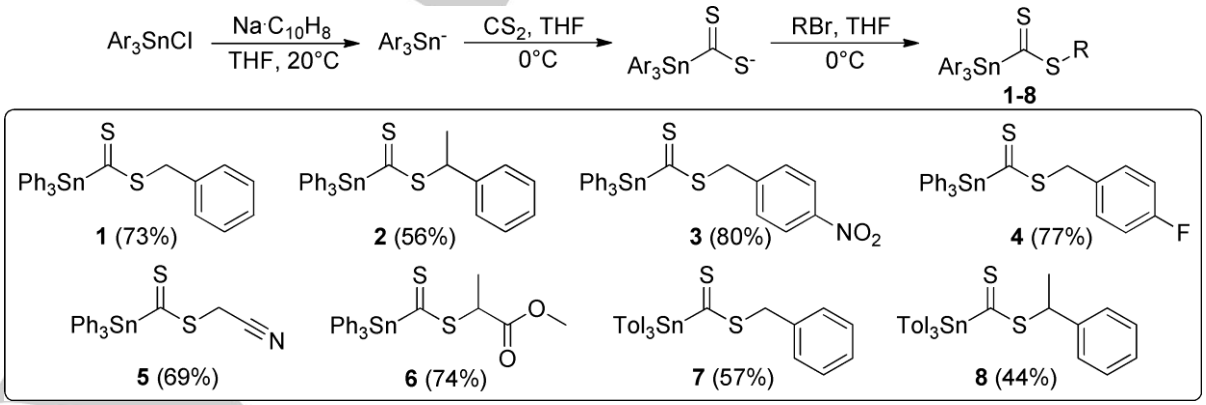

Scheme 2. Synthesis and structures of compounds **1**-**8**. Numbers in parentheses represent overall yields after purification.

10.1002/chem.201703412

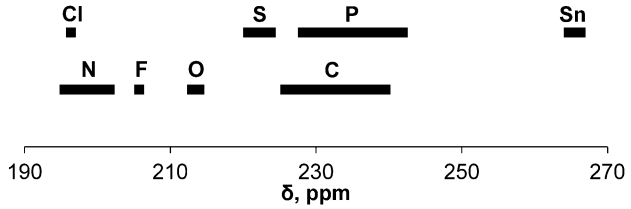

Figure 1. ^{13}C NMR chemical shifts of thiocarbonyl groups of selected thiocarbonylthio compounds and title triarylstannanecarbodithioates.[17,18,20,40–48]

The ^{119}Sn NMR chemical shift values (Figures S3, S6, S9, S12, S16, S19, S22 and S25) obtained for RAFT agents **1**-**8** fall in a narrow range between δ = -179.5 (**5**) and -192.7 ppm (**3**) and show slight differences in chemical shift depending on the nature of the *S*-alkyl substituent. Tri-*p*-tolylstannanecarbodithioates **7** and **8** have about 10 ppm higher chemical shift values than corresponding triphenylstannanecarbodithioates **1** and **2** due to electron-donating effect of *p*-tolyl groups.[32] Finally, the ^{19}F NMR spectrum of **4** (Figure S13) consists of a singlet with chemical shift of -115.6 ppm. The IR spectra exhibit characteristic stretching bands for the thiocarbonyl bonds in the range of expected values for C=S bonds involved in a free CS_2 group[19,20,30,35,36,38] with wavenumbers of 1040.5–1050.0 cm^{-1}.

According to the RAFT polymerization mechanism (Scheme 3), the efficiency of RAFT agents is affected by R and Z substituents.[49] The R group must be a good homolytic leaving group that is able to reinitiate the polymerization at a similar rate to that of propagation.[50] The Z group determines the stability of the intermediate radical and the reactivity of the C=S bond towards radical addition.[45]

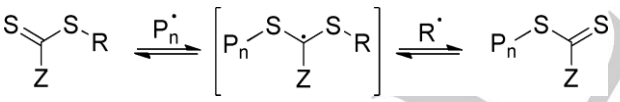

Scheme 3. Main equilibrium of RAFT polymerization.

Monomers can be divided into two groups: “more activated monomers” (MAMs) which give propagating radicals with relatively low reactivity in radical addition due to the enhanced electronic stabilization and steric factors; and “less activated monomers” (LAMs) which generate more reactive macroradicals.[51] MAMs are well controlled by active RAFT agents such as dithioesters or trithiocarbonates whereas LAMs require less active RAFT agents such as xanthates or dithiocarbamates.[6] Attempts to use activated RAFT agents to control the polymerization of LAMs generally result in complete inhibition of polymerization, as poly(LAM) macroradicals are relatively poor leaving groups, which disables the fragmentation process. By contrast, less active RAFT agents provide a moderate level of control over the polymerization of such MAMs as acrylamides and acrylates.

Typical less activated RAFT agents—xanthates and dithiocarbamates—demonstrate the lowest chemical shifts of thiocarbonyl group in ^{13}C NMR due to the conjugation of lone pairs of oxygen or nitrogen with thiocarbonyl group. More activated RAFT agents, namely trithiocarbonates, dithioesters and phosphoryl(thio)methanedithioates have much higher chemical shifts. These factors suggest that the chemical shift of the thiocarbonyl carbon can be used for the rough evaluation of activity of RAFT agents. According to this hypothesis, benzyl chloro- and fluorodithioformates[17] should be efficient in the polymerization of LAMs (Figure 1). Following the same reasoning, triarylstannanecarbodithioates should be efficient in the polymerization of MAMs.

Crystal structures

There are limited data on the crystal structures of triarylstannanecarbodithioates.[30,36,38] Up to this time only structures of four compounds, namely benzyl, methyl and triphenylstannyl triphenylstannanecarbodithioate **1**,[36] **9**[30] and **10**,[38] respectively, and tri-*p*-tolylstannyl tri-*p*-tolylstannane-carbodithioate **11**,[38] were reported. However, the Cambridge Structural Database[52] entries of compounds **1** and **9** contain some inaccuracies. Based on these facts it was decided to repeat these two analyses in parallel with determination of crystal structures of compounds **2**-**8**. For this purpose, methyl triphenylstannanecarbodithioate **9** was prepared in good yield according to our synthetic procedure. Its NMR spectra (Figures S27-S29) and other physical properties are in good agreement with previously published data.[30]

While attempts to crystallize compound **6** were unsuccessful, pink crystals of the other eight products allowed us to obtain good quality X-Ray structures. The molecular structures of **1**-**5** and **7**-**9** are very similar (Figures 2, S30-S37). They all crystallize in the $P\bar{1}$ space group except compound **7** which crystalizes in $P2_1$ space group with 4 molecules in the asymmetric unit and compound **9** (space group $P\bar{4}\,2_1c$ with ¼ molecule in the asymmetric unit) (Table S1). Crystals of the compound **9** have a structure similar to that of tetraphenylstannane[53] (tetragonal with $\bar{4}$ symmetry) in which the carbodithioate group and the phenyl ring are disordered over the same sites by symmetry with occupancies 0.25:0.75. Depending on the constraints or restraints used to refine the structure, the bond lengths and angles might be slightly different and only one command was used (ISOR) to model the structure.

The geometric parameters of their crystal structures are listed in Tables S2-S17, while selected bond lengths (Å) and angles (°) of planar $SnCS_2$ fragment for compounds **1-5**, **7,9** and compounds **10** ,**11**[38] are collected in Table 1. Most of the bond lengths and angles are similar, although the Sn-C and C=S bonds of compound **3** are unusually short, while the C-S single bond is elongated. These observations can be explained by the effect of the strongly electron withdrawing nitro group. At the same time, the weakly electron withdrawing fluorine in compound **4** has no visible effect on bond lengths.

10.1002/chem.201703412

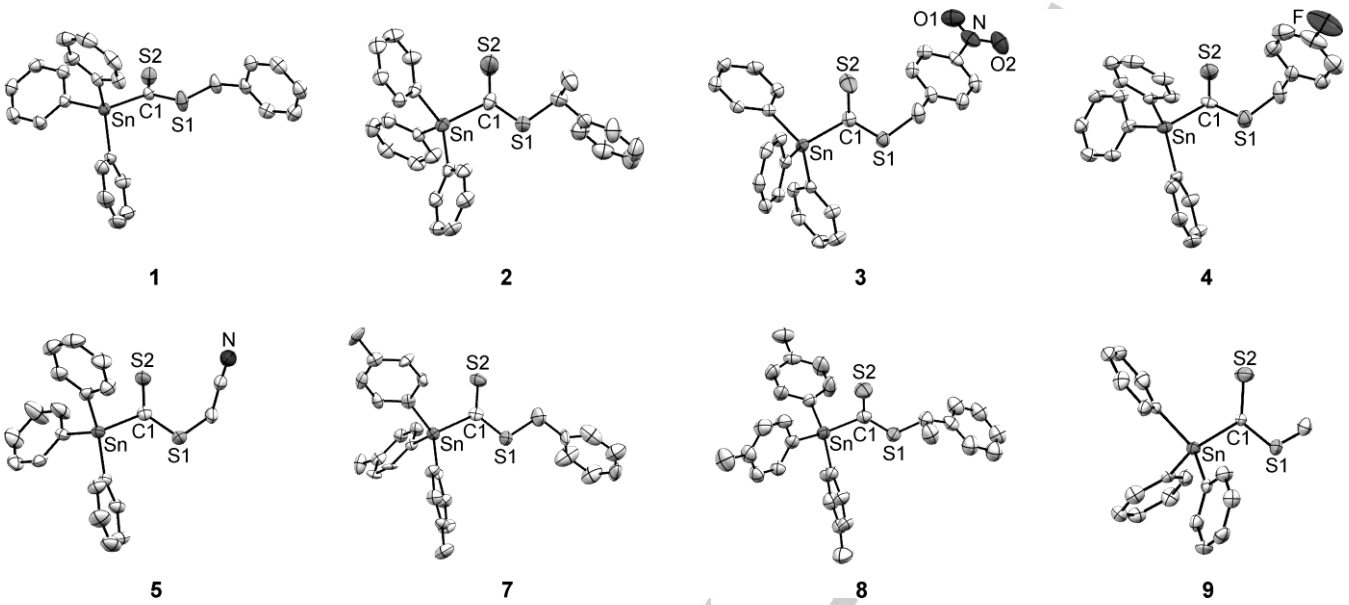

Figure 2. Simplified molecular views of compounds **1**-**5**,**7**-**9**. Thermal ellipsoids represent 50% probability; hydrogens and disordered atoms are omitted for clarity.

Table 2 summarizes selected bond lengths and angles for the central fragment of selected thiocarbonylthio compounds **12**-**21** with variation of Z-group structure.[20,54–60] Key bond lengths and angles are similar for the listed compounds, but more active RAFT agents, namely trithiocarbonates, dithioesters and phosphorylmethanedithioates have shorter C=S double bonds (between 1.614 Å for trithiocarbonate **18** and 1.649 Å for dithioester **17**) that are similar to those of the triarylstannanecarbodithioates **1**-**5** and **7**-**9** (1.60-1.64 Å). Less active RAFT agents such as dithiocarbamates **14** and **15** have longer C=S bond (1.68-1.70 Å). Moreover, the C-S bond length is shorter for more active RAFT agents, particularly for phosphorylmethanedithioates. The phosphorylmethanedithioate **20** has the smallest Z-C=S angle (120.2°) of RAFT agents that falls in the range of the values observed for triarylstannanecarbodithioates **1**-**5**, **7**-**9** (117.5-123.7°).

But the main finding is the correlation between the Z-C bond (Table 2) and the chemical shift of the carbon of the thiocarbonyl (Figure 1). The compounds fall into three distinct groups: first N, Cl, F and O, then S, C and P, and finally tin. The longer the bond, the higher the chemical shift. This decrease of electron density reflects the polarity of the bond which has a direct influence on radical addition to the RAFT agent during polymerization (Scheme 3).

Table 1. Selected bond lengths (Å) and angles (°) for the $SnCS_2$ fragment for the compounds **1**-**5** and **7**-**11**.

compound	**1**	**2**	**3**	**4**	**5**	**7**[a]	**8**	**9**	**10**[38]	**11**[38]
Sn-C	2.189	2.191	2.155	2.181	2.185	2.193	2.204	2.165	2.161	2.187
C=S	1.629	1.626	1.608	1.626	1.624	1.619	1.622	1.641	1.632	1.619
C-S	1.709	1.681	1.767	1.719	1.718	1.694	1.703	1.670	1.714	1.656
Sn-C=S	122.37	117.77	123.76	118.27	118.43	119.01	120.78	122.0	119.3	117.5
Sn-C-S	111.96	114.52	110.92	114.35	116.54	113.75	110.22	114.3	117.4	116.1
S=C1-S	125.66	127.71	125.26	127.38	125.02	127.03	128.95	123.1	123.3	126.4

[a]average values for four molecules in the asymmetric unit

Table 2. Selected bond lengths (Å) and angles (°) for the central fragment of common thiocarbonylthio compounds according to the literature data.[20,54–60]

compound	**1**	**12**[54]	**13**[55]	**14**[56]	**15**[56]	**16**[57]	**17**[58]	**18**[59]	**19**[60]	**20**[20]	**21**[20]
Z-group	$SnPh_3$	OEt	OEt	NEt_2	Morpholine	Ph	Ph	$S(CH_2)_2CO_2H$	$SCMe_2CO_2H$	$P(O)Ph_2$	$P(O)(NiPr_2)_2$
Z-C	2.189	1.313	1.332	1.288	1.318	1.481	1.487	1.746	1.746	1.848	1.868
C=S	1.629	1.642	1.636	1.68	1.702	1.632	1.649	1.614	1.630	1.635	1.634
C-S	1.709	1.756	1.759	1.788	1.743	1.745	1.732	1.742	1.748	1.710	1.720
Z-C=S	122.37	127.89	127.40	125.09	122.58	123.62	123.48	126.14	126.75	120.25	124.97
Z-C-S	111.96	105.65	106.41	113.75	118.11	113.50	113.01	106.51	106.90	109.55	108.49
S=C-S	125.66	126.46	126.19	121.15	121.30	122.88	123.51	127.34	126.32	130.17	126.51

Table 3. Results of Sn-RAFT mediated polymerizations.

Entry	RAFT agent	M[a]	Time h	M conv[b]	$M_{n\,th}$[c] kg mol^{-1}	M_n[d] kg mol^{-1}	$Đ$[e]
1	**1**	BA	0.5	1.17%	0.77	ND[f]	ND
2	**1**	BA	1	3.93%	1.37	1.44	1.23
3	**1**	BA	2	38.17%	8.83	9.73	1.07
4	**1**	BA	3.5	70.93%	15.97	18.11	1.06
5	**1**	BA	5	84.57%	18.94	22.28	1.08
6	**1**	BA	8	93.81%	20.96	24.84	1.10
7	**2**	BA	0.5	1.7%	0.89	ND	ND
8	**2**	BA	1	2.7%	1.12	ND	ND
9	**2**	BA	2	17.3%	4.31	4.78	1.16
10	**2**	BA	3.5	51.4%	11.73	14.30	1.07
11	**2**	BA	5	72.4%	16.31	20.31	1.07
12	**2**	BA	8	89.5%	20.04	24.59	1.10
13	**3**	BA	0.5	1.2%	0.82	ND	ND
14	**3**	BA	1	2.0%	0.99	ND	ND
15	**3**	BA	2	13.1%	3.41	3.48	1.14
16	**3**	BA	3.5	35.7%	8.35	9.29	1.07
17	**3**	BA	5	51.0%	11.67	13.59	1.06
18	**3**	BA	8	67.3%	15.22	18.01	1.08
19	**4**	BA	0.5	0.9%	0.73	ND	ND
20	**4**	BA	1	5.7%	1.78	1.56	1.18
21	**4**	BA	2	52.5%	11.96	13.28	1.06
22	**4**	BA	3.5	78.9%	17.72	19.97	1.06
23	**4**	BA	5	88.0%	19.70	22.65	1.09
24	**4**	BA	8	93.7%	20.95	24.79	1.13
25	**7**	BA	0.5	1.0%	0.77	ND	ND
26	**7**	BA	1	7.5%	2.20	2.13	1.25
27	**7**	BA	2	44.3%	10.21	10.15	1.07
28	**7**	BA	3.5	76.8%	17.29	18.13	1.06
29	**7**	BA	5	86.1%	19.33	21.02	1.08
30	**7**	BA	8	94.1%	21.05	23.50	1.09
31	**8**	BA	0.5	1.5%	0.91	ND	ND
32	**8**	BA	1	4.2%	1.50	1.12	1.18
33	**8**	BA	2	22.5%	5.46	5.67	1.09
34	**8**	BA	3.5	47.0%	10.82	11.56	1.06
35	**8**	BA	5	65.0%	14.74	16.20	1.06
36	**8**	BA	8	84.8%	19.05	21.05	1.07
37	**1**	St	2	2.2%	0.98	1.16	1.18
38	**1**	St	4	5.1%	1.59	1.68	1.24
39	**1**	St	8	10.3%	2.67	2.82	1.31
40	**1**	St	24	28.9%	6.54	9.07	1.28
41	**1**	St	48	46.4%	10.18	18.46	1.36
42	**1**	St	72	55.8%	12.15	25.36	1.42
43	**7**	St	2	0.9%	0.75	1.21	1.18
44	**7**	St	4	1.5%	0.86	1.48	1.24
45	**7**	St	8	4.4%	1.47	2.18	1.33
46	**7**	St	24	19.5%	4.61	8.01	1.32
47	**7**	St	48	36.0%	8.05	16.51	1.34
48	**7**	St	72	43.7%	9.66	20.08	1.44

[a]Monomer. [b]Monomer conversion determined by ^{1}H NMR.
[c]$M_{n\,th} = M_w$(RAFT agent) + ([M]$_0$/[RAFT agent]$_0$)×(conv.)×M_w(M).
[d]Determined by SEC. [e]$Đ = M_w/M_n$. [f]Not determined.

RAFT polymerizations

To evaluate the structure-reactivity relationships for the alkyl triarylstannanecarbodithioates, the RAFT polymerization of *n*-butyl acrylate (BA) was performed in the presence of RAFT agents **1**-**4**, **6** and **7** at 60°C with AIBN as thermal initiator (Scheme 4). Additionally, compounds **1** and **7** were studied in the polymerization of styrene (St). The initial reactant ratios [BA]:[CTA]:[AIBN] = 170:1:0.2 and [St]:[CTA]:[AIBN] = 200:1:0.2 were chosen so that the theoretical number-average molar masses ($M_{n\,th}$) of the polymers at full conversion were around 20 kg mol^{-1}. Selected conversion-time data, number-average molecular weights and dispersities of obtained polymers are summarized in Table 3.

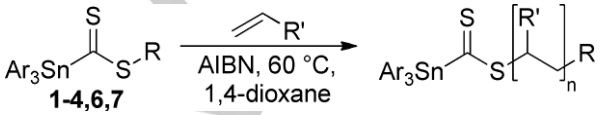

Scheme 4. Sn-RAFT polymerization.

In the case of BA polymerization, a 1 hour inhibition period was observed for all RAFT agents (Figure 3). This phenomenon is related to the very high reactivity of Sn-RAFT agents with slow initialization.[26] The structure of the R-group has a clear effect on the rate of polymerization, whereas the substitution of Z-group does not have a significant effect. Hence, **1**,**4** and **7** with benzyl or 4-fluorobenzyl R-groups provide the highest rates of polymerization, consistent with the stability of the benzyl radical, which is scarcely affected by a *para*-fluoro substituent. In case of more stabilized secondary 1-phenylethyl radical (**2** and **8**) the polymerization is slightly slower. Finally, significant resonance stabilization of the 4-nitrobenzyl radical in the case of **3** slows down the reinitiation and the polymerization in general.

For all the RAFT agents tested, M_n values (Figure 3) increase linearly during the polymerization in agreement with theoretical predictions. However, a slight upward curvature can be observed at higher conversions due to chain termination via recombination. Dispersities (Figure 3) decrease continuously over the course of the polymerization, reaching a minimum of 1.06 before slightly increasing (up to 1.13 in the worst case with RAFT agent **4**) after about 75% conversion due to irreversible deactivation of a small fraction of growing chains. These features are illustrated by the evolution of the SEC chromatograms of PBA samples (Figures 3, S38-S42). Slight shouldering can be observed at high reaction times due to formation of dead chains with doubled molecular weight.

RAFT agents **1** and **7** showed similar levels of control over the polymerization of styrene, as well as quite similar polymerization kinetics (Figure S43), though the reaction was slightly faster in the presence of **1**. M_n values (Figure S44) agreed with theory only at the initial stage of the polymerization, with strong deviations at higher reaction times, while $Đ$ increased from 1.18 to 1.44. SEC analysis (Figures S45 and S46) showed the formation of multimodal molecular weight distributions. Such behavior may be

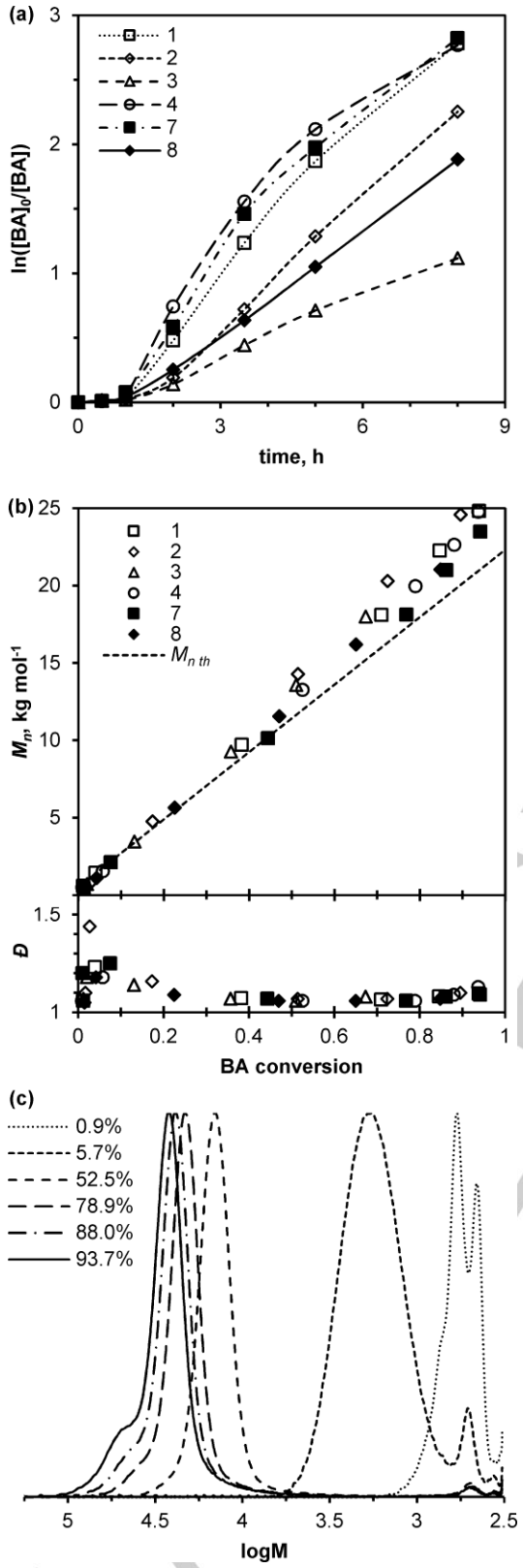

Figure 3. Results of Sn-RAFT polymerizations of BA. (a) semi-logarithmic kinetic plot, (b) evolution of M_n and $Đ$, (c) overlay of SEC chromatograms for CTA **4**.

due to thermal degradation of triarylstannanecarbodithioates, which becomes significant over the long reaction times required for St polymerization.

The chemical structure of RAFT agent **4** allows both ^{19}F and ^{119}Sn NMR to be used as separate analytical channels to study the transformations of *α*- and *ω*-functionalities respectively over the course of polymerization.

For this purpose, polymerizations of BA and St were performed directly in NMR tubes[25] with C_6D_6 as a solvent and trifluorotoluene as an internal standard for ^{19}F NMR quantification of RAFT agent transformations. It should be noted that ^{19}F NMR is quantitative, whereas ^{119}Sn NMR taken with proton decoupling can be used only for qualitative evaluation due to the heteronuclear Overhauser effect.

For each monomer, 6 parallel experiments were performed (Table 4). The concentration of RAFT agent was increased to enhance the quality of ^{119}Sn NMR spectra. The initial concentration ratio of reagents was [Monomer]:[RAFT agent **4**]:[AIBN] = 60:1:0.1 corresponding to maximum $M_{n\ th}$ values of 8.22 kg mol^{-1} for BA and 6.79 kg mol^{-1} for St. To guarantee uniformity of initial composition, all tubes in the series were prepared in a glovebox from the same degassed stock solution. After heating for the requisite times, reaction mixtures were quenched by freezing in liquid nitrogen, then ^1H, ^{19}F and ^{119}Sn NMR spectra were collected (Figures S47-S58), and, finally, the contents of each tube were analyzed by SEC.

Table 4. Results of the polymerizations using **4** as CTA with NMR monitoring.

Entry	Time h	M[a]	M conv[b]	RAFT conv[c]	$M_{n\ th}$[d] kg mol^{-1}	M_n[e] kg mol^{-1}	$Đ$[f]
1	0.5	BA	1.5%	18.1	0.65	ND[g]	ND
2	1	BA	2.8%	33.0	0.75	ND	ND
3	2	BA	6.8%	56.1%	1.06	ND	ND
4	4	BA	37.7%	93.7%	3.44	3.49	1.19
5	5	BA	55.3%	98.3%	4.79	4.46	1.17
6	6	BA	75.7%	99.9%	6.35	6.61	1.12
7	1	St	1.1%	5.9%	0.61	ND	ND
8	2	St	3.4%	32.6%	0.75	ND	ND
9	6	St	6.2%	46.2%	0.92	ND	ND
10	12	St	9.7%	58.3%	1.14	ND	ND
11	24	St	16.5%	74.0%	1.57	1.18	1.29
12	48	St	29.4%	87.9%	2.37	2.23	1.33

[a]Monomer. [b]Monomer conversion determined by ^1H NMR.
[c]RAFT agent conversion determined by ^{19}F NMR.
[d]$M_{n\ th} = M_w$(RAFT agent) + ([M]$_0$/[RAFT agent]$_0$)×(conv.)×M_w(M).
[e]Determined by SEC. [f]$Đ = M_w/M_n$. [g]Not determined.

The combination of ^1H and ^{19}F NMR allowed precise quantification of the conversions of monomers and RAFT agent. The corresponding kinetic plots are shown in Figures S59 and S60. In BA polymerization, the retardation period lasts only up to about 50 % RAFT agent conversion (Figure S59). Then polymerization continues with gradual consumption of RAFT agent, indicating non-selective initialization. No induction period was observed in St polymerization (Figure S60). These data allowed determination of apparent C_{tr} values of 12.3 for BA and

8.5 for St (95% confidence intervals 9.6<C_{tr}<15.0 for BA and 6.4<C_{tr}<10.8 for St) using non-linear least squares fitting[61] (Figure 4).

During the polymerization process, no signals outside of the -120 to -115 ppm region were observed in ^{19}F NMR spectra (Figures S47-S56). In the case of BA polymerization (Figures 5, S47), in parallel with decrease of initial RAFT agent peak at -115.9 ppm, two other peaks arise with chemical shifts of -118.2 ppm and about -118.7 ppm. The first peak can be attributed to the monoadduct as it arises only at the initial step of the polymerization and subsequently disappears completely, reaching a maximum concentration of 13.2 % after 2 hours. Additionally, its appearance as well-defined peak confirms that this signal belongs to a small molecule. The broad peak at -118.7 ppm belongs to the polymer's *α*-chain end. However, ^{19}F NMR spectroscopy with proton decoupling reveals a set of separate peaks which can be attributed to oligomers. Two of them with chemical shifts of -118.5 and -118.6 ppm are particularly interesting as they appear only in parallel with the peak of monoadduct and can be very likely attributed to bis- and triadduct.

Observation of all these peaks confirms the non-selective RAFT agent initialization. Finally, the intensity of polymer peak after 8 hours confirms the complete transformation of RAFT agent into polymer.

The evolution of M_n and $Đ$ (Figures S61-S64) follows the same trends as in the case of RAFT polymerization under classical conditions. However, there is a small improvement in the control that is mostly explained by increased concentration of RAFT agent.

Detailed examination of ^{19}F and ^{119}Sn NMR spectra (Figures 5 and 6) reveals some intriguing details of RAFT agent transformations.

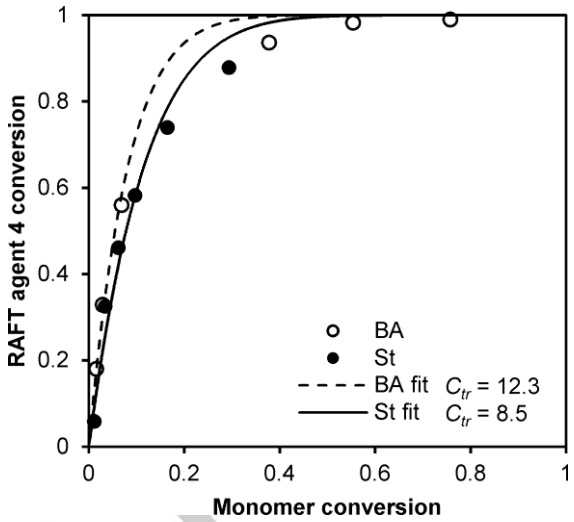

Figure 4. Determination of C_{tr} for the polymerization of BA and St mediated by RAFT agent **4** based on ^{1}H and ^{19}F NMR data.

^{119}Sn NMR spectra (Figures 6, S51, S52) demonstrate similar tendencies as were previously observed for methyl acrylate.[25] A characteristic drift of the chemical shift towards weaker field was observed, whereas the chemical shift of the polyacrylate macroRAFT agent is close to that of RAFT agent **6** with acrylate-like R-group. Additionally, a sharp peak with a chemical shift of -186.1 ppm was observed at the initial step of the polymerization. Its disappearance after 2 hours suggests that it is due to a monoadduct. After 8 hours, a new peak was observed around -52 ppm. In our previous study[25] this was identified as

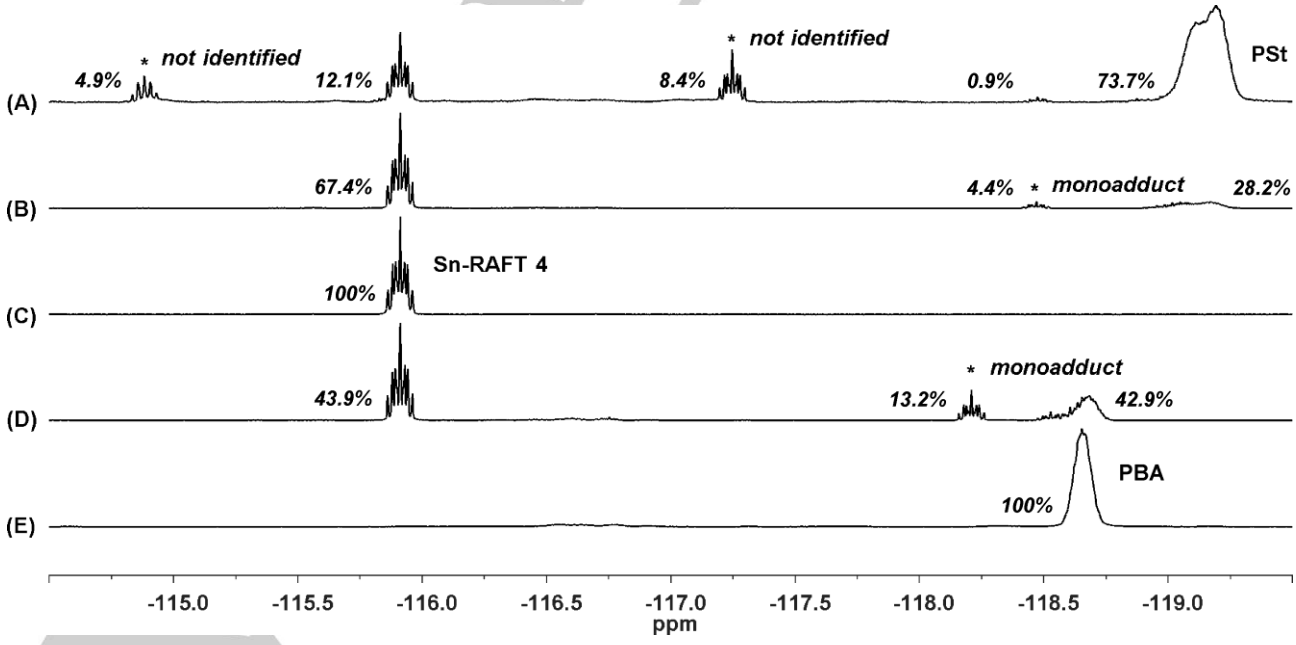

Figure 5. ^{19}F NMR spectra of reaction mixtures of: St with Sn-RAFT **4** after 48 h (A) and 2 h (B); Sn-RAFT 4 (C); reaction mixtures of BA with Sn-RAFT **4** after 2 h (D) and 6 h (E). Each spectrum is fitted to highest intensity. Numbers next to each peak describe the percent fraction of each species in solution.

10.1002/chem.201703412

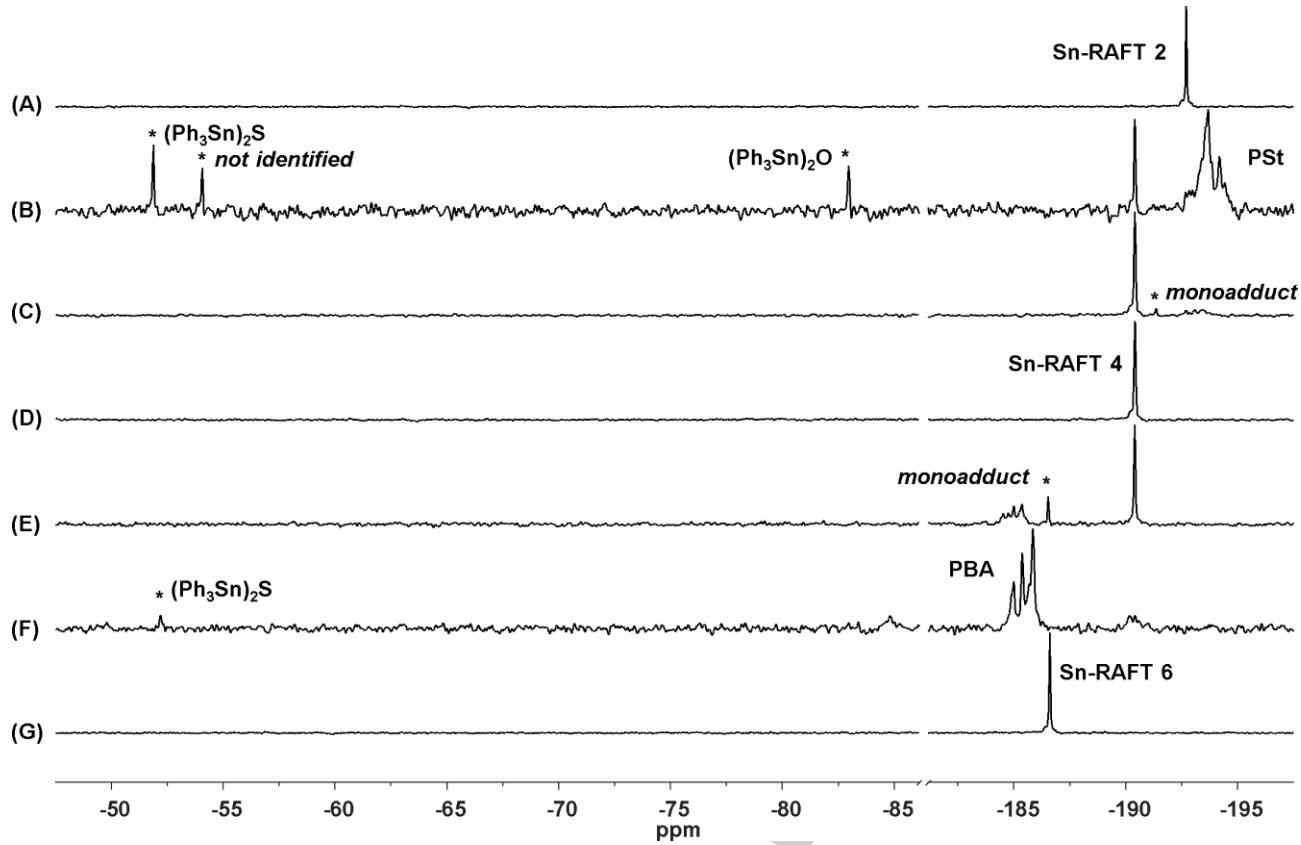

Figure 6. $^{119}Sn\{^1H\}$ NMR spectra of: Sn-RAFT **2** (A); reaction mixtures of St with Sn-RAFT **4** after 48 h (B) and 2 h (C); Sn-RAFT 4 (D); reaction mixtures of BA with Sn-RAFT **4** after 2 h (E) and 6 h (F); Sn-RAFT **6** (G). Each spectrum is fitted to highest intensity.

bis(triphenylstannyl)sulfide, a product of thermal decomposition of the polymer's *ω*-chain ends. We believe that such loss of polymer chains is the main driving force for the observed deviations of the control over molecular weight and shouldering in SEC chromatograms at higher reaction times.

In case of St polymerization, ^{19}F NMR spectra (Figures S53-S56) demonstrate the same trends as in the case of BA. Incorporation of St units between 4-fluorobenzyl group and triphenylstannanecarbodithioate moiety leads to the gradual drift of the fluorine signal to higher field, while differences in the chemical shifts allow identification of the monoadduct at -118.5 and higher adducts between -118.96 and -119.03 ppm. However, the most remarkable point is the formation of two new peaks at -117.2 and -114.9 ppm after 6 hours of the polymerization. Based on their appearance, they belong to small molecules and, hypothetically, should belong to the products of thermal decomposition of initial RAFT agent which was not yet transformed into polymer as ^{19}F NMR shows only the evolution of R-group. At the same time, ^{119}Sn NMR spectra (Figures 6, S57, S58) allow detection of the decomposition of both initial RAFT agent and polymer's *ω*-chain end. After 48 hours of the polymerization, the NMR spectrum reveals three new species in addition to the signals of unreacted **4** and polystyrene macroRAFT agent. Two of them were identified as bis(triphenylstannyl) sulfide and bis(triphenylstannyl) oxide,[25] while the compound with a chemical shift of -54.1 ppm remains unidentified. The kinetics and mechanism of this thermal degradation is currently under investigation.

Conclusions

New alkyl triarylstannanecarbodithioates (Sn-RAFT agents) were synthesized using a simple procedure from triarylstannyl chlorides. Their complete characterization using spectroscopic and spectrometric methods, including X-ray analyses, was described. The structures obtained were very similar and most of the compounds crystallize in the $P\bar{1}$ space group. For the first time, the chemical shift in ^{13}C NMR and the bond length of C=S for the main classes of thiocarbonylthio RAFT agents were discussed and compared to those of Sn-RAFT agents. The very high chemical shift (262-266 ppm) of C=S compared to other types of RAFT agents and bond lengths similar to those of highly reactive dithioesters and trithiocarbonates indicated a high reactivity of alkyl triarylstannanecarbodithioates in RAFT polymerization. Indeed, they were found to control efficiently the RAFT polymerization of St and BA. The effect of R and Z groups of Sn-RAFT agents on the kinetics of polymerization of St has been discussed. In most cases, M_n increases with monomer conversion with a strong upward deviation over the course of the

polymerization, with final dispersities around 1.4. The polymerization of BA proceeds with a much better control over M_n values and lower dispersities ($Đ$ < 1.15). High C_{tr} values of 8.5 and 12.3 have been determined for St and BA, respectively, using ^{1}H and ^{19}F NMR spectroscopy. ^{119}Sn and ^{19}F NMR revealed the presence of an initialization period during BA (but not St) polymerization. It also allowed the identification of di(triphenylstannyl) oxide and di(triphenylstannyl) sulfide among the by-products, which may explain the deviations from a well-controlled polymerization. The Sn-RAFT chain end appears to be thermally unstable, and degrades over prolonged reaction times. Nevertheless, Sn-RAFT polymerization is one of the few examples of a RDRP process where heteronuclear NMR allows observation of an initialization step, determination of chain transfer constants and the revelation and identification of RAFT agent decomposition products.

Experimental Section

General: All the reactions were performed using standard Schlenk techniques involving flame-dried glassware, oven-dried Teflon coated stir bars and sleeve stopper septa under a dry argon atmosphere. Terumo single use plastic syringes were used for the measurements of all liquid reagents and solvents. Air and moisture-sensitive solids were weighed in a glovebox under a dry argon atmosphere. Products were purified with flash chromatography on 35–70 mesh silica gel (porosity 90 Å) using degassed eluents and positive pressure of argon.

Melting points were measured with a sealed capillary by using the Stuart automatic melting point SMP40 apparatus. NMR spectra were recorded using a Bruker Avance AMX 300 spectrometer (strength of the magnetic field is 7.049 T, operating frequencies are 300.13 MHz for ^{1}H, 282.40 MHz for ^{19}F, 98.20 MHz for ^{119}Sn and 75.47 MHz for ^{13}C) at 298 K. Chemical shifts are expressed in parts per million with residual solvent signals as internal reference (^{1}H and ^{13}C{^{1}H} NMR). The external chemical shift reference is Me_4Sn (0 ppm) for ^{119}Sn NMR and trifluorotoluene (-63.72 ppm) for ^{19}F NMR. IR spectra were recorded using a Thermo Fischer Nexus 6700 FTIR spectrometer in ATR mode, values of ν_{max} (in cm^{-1}) are given for the major absorption bands. High resolution mass spectrometry (HRMS) was performed on Waters GCT Premier CAB109 TOF mass spectrometer in the chemical ionisation mode (CH_4).

The monomer conversions were determined by ^{1}H NMR spectroscopy. Number-average molar mass (M_n) and dispersity ($Đ$) values of the polymer samples were determined by SEC. The SEC analyses were conducted on a system composed of Waters 515 HPLC pump, Agilent 1260 Autosampler, Varian ProStar 500 column valve module, set of three Waters columns (Styragel Guard Column, 20 µm, 4.6 mm × 30 mm, Styragel HR3, 5 µm, 7.8 mm × 300 mm and Styragel HR4E, 5 µm, 7.8 mm × 300 mm), Varian ProStar 325 UV-Vis detector set at 290 nm and Wyatt Optilab rEX differential refractive index detector using tetrahydrofuran (THF) as an eluent at a flow rate of 1.0 mL min^{-1} (35 °C). The column system was calibrated with PSt standards (ranging from 860 to 483400 g mol^{-1}) for PSt and PMMA standards (ranging from 1120 to 138600 g mol^{-1}) for PBA using the Landau-Kuhn-Mark-Houwink-Sakurada equation.[62] Prior to injection, samples were diluted to a concentration about 5 mg mL^{-1} and filtered through 0.45 µm Nylon syringe filters.

Materials: Solvents were received from Sigma-Aldrich, Alfa Aesar or SDS and dried, if necessary, by passing through a column packed with activated molecular sieves 4 Å under a positive pressure of dry nitrogen. Benzyl bromide (Acros, 98%), bromoacetonitrile (Aldrich, 97%), (1-bromoethyl)benzene (Aldrich, 97%), 4-bromotoluene (Aldrich, 98%), 4-fluorobenzyl bromide (Aldrich, 97%), iodomethane (Aldrich, ≥99%), magnesium (Aldrich, 98%), Na metal (Aldrich), methyl 2-bromopropionate (Alfa Aesar, 97%) naphtalene (Aldrich, ≥99%), 4-nitrobenzyl bromide (Aldrich, 99%), tin(IV)chloride (Aldrich, 98%) and triphenylstannyl chloride (Fluka, 95%) were used as received. Tri-*p*-tolylstannyl chloride was prepared in two steps according to the literature methods.[63,64] Butyl acrylate (BA, Aldrich, 99%) and styrene (St, Aldrich, 99%) were passed through a column filled with neutral aluminium oxide (Brockmann I) prior to use. 2,2'-Azobis(2-methylpropionitrile) (AIBN, Acros, 98%) was purified by double recrystallization from methanol.

General method for the synthesis of compounds 1-9. A solution of naphthalene (2.56 g, 20 mmol) in dry THF (50 mL) was stirred with Na metal (0.46 g, 20 mmol) at ambient temperature for 4 h. Obtained dark green solution was slowly added at ambient temperature (*Caution! Reaction is highly exothermic*) to the corresponding triarylstannyl chloride (10 mmol) with vigorous stirring and stirred for additional 1 h. Then CS_2 (2 mL, 33 mmol) was added dropwise to the orange solution of (triarylstannyl)sodium at 0-5 °C and stirred for 1 h. Final solution of crude sodium triarylstannanecarbodithioate was adjusted to 100 mL with dry THF (0.1 M concentration) and used for the next synthetic steps as it is.

Sodium triarylstannanecarbodithioate solution (50 mL, 5 mmol) was added dropwise to the corresponding alkyl halide (6 mmol) at 0-5 °C with vigorous stirring and stirred additionally for 2 h. Then it was concentrated under a reduced pressure and washed twice with 20 mL of cold hexane to remove naphthalene and most of impurities. Red oily residue was subjected to chromatography, eluting with a petroleum ether – ethyl acetate gradient to collect the pink fraction. After the concentration under a reduced pressure, the pink oil was crystalized from corresponding solvent (hexane for **1,2,5**,**6** acetone for **3,4** or pentane for **7,8**).

Benzyl triphenylstannanecarbodithioate **1**[25] (1.89 g, 73%). Pink crystals, m.p.: 94–96 °C (lit. 96 °C[35]). ^{1}H NMR (300.13 MHz, toluene-d$_8$, 298 K): 4.43 (pt, $^{4}J_{Sn,H}$ = 4.2 Hz, 2H; C$\underline{H}_2$C$_6$H$_5$), 6.93 (m, 5H, CH$_2$C$_6\underline{H}_5$), 7.09–7.19 (m, 9H; 3-H, 4-H, (C$_6\underline{H}_5$)$_3$Sn), 7.57–7.81 (m, ^{3}J$_{Sn,H}$ = 50.7 Hz, 6H; 2-H, (C$_6\underline{H}_5$)$_3$Sn); ^{13}C{^{1}H} NMR (75.47 MHz, toluene-d$_8$, 298 K): 38.8 (pt, $^{3}J_{Sn,C}$ = 12.4 Hz; $\underline{C}$H$_2$C$_6$H$_5$), 127.5 (s; 3-C, CH$_2\underline{C}_6$H$_5$), 128.7 (s; 4-C, CH$_2\underline{C}_6$H$_5$), 129.1 (pt, $^{2}J_{Sn,C}$ = 55.9 Hz; 2-C, ($\underline{C}_6$H$_5$)$_3$Sn), 129.5 (s; 2-C, CH$_2\underline{C}_6$H$_5$), 129.8 (pt, $^{4}J_{Sn,C}$ = 12.1 Hz; 4-C, ($\underline{C}_6$H$_5$)$_3$Sn), 135.7 (s; 1-C, CH$_2\underline{C}_6$H$_5$), 137.4 (pt, $^{3}J_{Sn,C}$ = 38.6 Hz; 3-C, ($\underline{C}_6$H$_5$)$_3$Sn), 137.8 (pt, $^{1}J_{Sn,C}$ = 548 Hz; 1-C, ($\underline{C}_6$H$_5$)$_3$Sn), 264.7 (s; $\underline{C}S_2$); ^{119}Sn{^{1}H} NMR (98.20 MHz, toluene-d$_8$, 298 K): −191.0. IR: 1046.6 (C=S). HRMS (CI, CH_4, *m/z* of [MH$^+$]): found — 515.0245, calculated for $C_{26}H_{23}S_2Sn$ — 515.0259.

1-Phenylethyl triphenylstannanecarbodithioate **2**.[25] (1.49 g, 56%). Pink crystals, m.p.: 93–95 °C. ^{1}H NMR (300.13 MHz, toluene-d$_8$, 298 K): 1.44 (m, $^{3}J_{H,H}$ = 7.1 Hz, $^{5}J_{Sn,H}$ = 3.5 Hz, 3H; CH(C$\underline{H}_3$)C$_6$H$_5$), 5.84 (m, ^{3}J$_{H,H}$ = 7.1 Hz, ^{4}J$_{Sn,H}$ = 7.3 Hz, 1H; C$\underline{H}$(CH$_3$)C$_6$H$_5$), 6.90–7.08 (m, 5H; CH(CH$_3$)C$_6\underline{H}_5$), 7.09–7.19 (m, 9H; 3-H, 4-H, (C$_6\underline{H}_5$)$_3$Sn), 7.57–7.81 (m, $^{3}J_{Sn,H}$ = 51.9 Hz, 6H; 2-H, (C$_6\underline{H}_5$)$_3$Sn); ^{13}C{^{1}H} NMR (75.47 MHz, toluene-d$_8$, 298 K): 20.0 (s; CH($\underline{C}$H$_3$)C$_6$H$_5$), 46.3 (pt, $^{3}J_{Sn,C}$ = 13.3 Hz; $\underline{C}$H(CH$_3$)C$_6$H$_5$), 127.6 (s; 4-C, CH(CH$_3$)$\underline{C}_6$H$_5$), 128.0 (s; 2-C, CH(CH$_3$)$\underline{C}_6$H$_5$), 128.8 (s; 3-C, CH(CH$_3$)$\underline{C}_6$H$_5$), 129.1 (pt, $^{2}J_{Sn,C}$ = 54.3 Hz; 2-C, ($\underline{C}_6$H$_5$)$_3$Sn), 129.8 (pt, $^{4}J_{Sn,C}$ = 12.1 Hz; 4-C, ($\underline{C}_6$H$_5$)$_3$Sn), 137.4 (pt, ^{3}J$_{Sn,C}$ = 38.6 Hz; 3-C, ($\underline{C}_6$H$_5$)$_3$Sn), 138.0 (pt, ^{1}J$_{Sn,C}$ = 546 Hz; 1-C, ($\underline{C}_6$H$_5$)$_3$Sn), 141.3 (s; 1-C, CH(CH$_3$)$\underline{C}_6$H$_5$), 264.0 (s, $\underline{C}S_2$); ^{119}Sn{^{1}H} NMR (98.20 MHz, toluene-d$_8$, 298 K): −192.7. IR: 1040.5 (C=S). HRMS (CI, CH_4, *m/z* of [MH$^+$]): found — 533.0482, calculated for $C_{27}H_{25}S_2Sn$ — 533.0420.

4-Nitrobenzyl triphenylstannanecarbodithioate **3** (2.70 g, 80%). Red crystals, m.p.: 141–143 °C. ^{1}H NMR (300.13 MHz, toluene-d$_8$, 298 K): 4.18 (s, 2H; C$_6$H$_4$C$\underline{H}_2$), 6.58 (m, $^{3}J_{H,H}$ = 8.8 Hz, $^{6}J_{Sn,H}$ = 4.5 Hz, 2H; 2-H, C$_6\underline{H}_4$CH$_2$), 7.13–7.22 (m, 9H; 3-H, 4-H, (C$_6\underline{H}_5$)$_3$Sn), 7.57 (m, $^{3}J_{H,H}$ = 8.8 Hz, $^{7}J_{Sn,H}$ = 4.5 Hz, 2H; 3-H, C$_6\underline{H}_4$CH$_2$), 7.60–7.82 (m, $^{3}J_{Sn,H}$ = 51.6 Hz, 6H; 2-H, (C$_6\underline{H}_5$)$_3$Sn); ^{13}C{^{1}H} NMR (75.47 MHz, toluene-d$_8$, 298 K): 37.2 (pt, $^{3}J_{Sn,C}$ = 12.4 Hz; C$_6$H$_4\underline{C}$H$_2$), 123.6 (s; 2-C, $\underline{C}_6$H$_4$CH$_2$), 129.3 (pt, $^{2}J_{Sn,C}$ = 54.8 Hz; 2-C, ($\underline{C}_6$H$_5$)$_3$Sn), 129.8 (s; 3-C, $\underline{C}_6$H$_4$CH$_2$), 130.1 (pt, $^{4}J_{Sn,C}$ = 12.2 Hz; 4-C, ($\underline{C}_6$H$_5$)$_3$Sn), 137.4 (pt, $^{3}J_{Sn,C}$ = 38.8 Hz; 3-C, ($\underline{C}_6$H$_5$)$_3$Sn), 137.5 (pt, $^{1}J_{Sn,C}$ = 547 Hz; 1-C, ($\underline{C}_6$H$_5$)$_3$Sn), 142.8 (s; 1-C, $\underline{C}_6$H$_4$CH$_2$), 147.3 (s; 4-C, $\underline{C}_6$H$_4$CH$_2$), 264.8 (s; $\underline{C}S_2$); ^{119}Sn{^{1}H} NMR (98.20 MHz, toluene-d$_8$, 298 K): −187.2. IR: 1044.0 (C=S). HRMS (CI, CH_4, *m/z* of [MH$^+$]): found — 564.0101, calculated for $C_{26}H_{22}NO_2S_2Sn$ — 564.0114.

4-Fluorobenzyl triphenylstannanecarbodithioate **4** (2.06 g, 77%). Pink crystals, m.p.: 141–143 °C. ^{1}H NMR (300.13 MHz, toluene-d_8, 298 K): 4.29 (s, 2H; $FC_6H_4C\underline{H}_2$), 6.48–6.62 (m, 2H; 2-H, $FC_6\underline{H}_4CH_2$), 6.65–6.75 (m, 2H; 3-H, $FC_6\underline{H}_4CH_2$), 7.11–7.24 (m, 9H; 3-H, 4-H, $(C_6\underline{H}_5)_3Sn$), 7.56–7.85 (m, $^{3}J_{Sn,H}$ = 51.0 Hz, 6H; 2-H, $(C_6\underline{H}_5)_3Sn$); $^{13}C\{^{1}H\}$ NMR (75.47 MHz, toluene-d_8, 298 K): 37.8 (pt, $^{3}J_{Sn,C}$ = 12.4 Hz; $C_6H_4\underline{C}H_2$), 115.5 (d, $^{2}J_{F,C}$ = 21.5 Hz; 3-C, $F\underline{C}_6H_4CH_2$), 129.1 (pt, $^{2}J_{Sn,C}$ = 55.8 Hz; 2-C, $(\underline{C}_6H_5)_3Sn$), 129.9 (pt, $^{4}J_{Sn,C}$ = 12.2 Hz; 4-C, $(\underline{C}_6H_5)_3Sn$), 131.1 (d, $^{3}J_{F,C}$ = 8.1 Hz; 2-C, $F\underline{C}_6H_4CH_2$), 131.4 (d, $^{4}J_{F,C}$ = 3.3 Hz; 1-C, $F\underline{C}_6H_4CH_2$), 137.4 (pt, $^{3}J_{Sn,C}$ = 38.7 Hz; 3-C, $(\underline{C}_6H_5)_3Sn$), 137.7 (pt, $^{1}J_{Sn,C}$ = 548 Hz; 1-C, $(\underline{C}_6H_5)_3Sn$), 162.4 (d, $^{1}J_{F,C}$ = 246 Hz; 4-C, $F\underline{C}_6H_4CH_2$), 265.0 (s; $\underline{C}S_2$); $^{119}Sn\{^{1}H\}$ NMR (98.20 MHz, toluene-d_8, 298 K): −190.4; $^{19}F\{^{1}H\}$ NMR (282.40 MHz, toluene-d_8, 298 K): −115.9. IR: 1050.0 (C=S). HRMS (CI, CH_4, *m/z* of $[MH^+]$):found — 537.0179, calculated for $C_{26}H_{22}FS_2Sn$ — 537.0169.

Cyanomethyl triphenylstannanecarbodithioate **5** (1.60 g, 69%). Pink crystals (unstable), m.p.: ~65 °C (decomposition). ^{1}H NMR (300.13 MHz, $CDCl_3$, 298 K): 4.23 (pt, $^{4}J_{Sn,H}$ = 2.3 Hz, 2H; $C\underline{H}_2CN$), 7.46–7.62 (m, 9H; 3-H, 4-H, $(C_6\underline{H}_5)_3Sn$), 7.64–7.85 (m, $^{3}J_{Sn,H}$ = 53.5 Hz, 6H; 2-H, $(C_6\underline{H}_5)_3Sn$); $^{13}C\{^{1}H\}$ NMR (75.47 MHz, $CDCl_3$, 298 K): 17.9 (pt, $^{3}J_{Sn,C}$ = 12.6 Hz; $\underline{C}H_2CN$), 114.4 (s; $CH_2\underline{C}N$), 129.2 (pt, $^{2}J_{Sn,C}$ = 57.1 Hz; 2-C, $(\underline{C}_6H_5)_3Sn$), 130.2 (pt, $^{4}J_{Sn,C}$ = 12.3 Hz; 4-C, $(\underline{C}_6H_5)_3Sn$), 136.4 (s; 1-C, $(\underline{C}_6H_5)_3Sn$), 137.1 (pt, $^{3}J_{Sn,C}$ = 38.6 Hz; 3-C, $(\underline{C}_6H_5)_3Sn$), 262.6 (s; $\underline{C}S_2$); $^{119}Sn\{^{1}H\}$ NMR (98.20 MHz, $CDCl_3$, 298 K): −179.5.

Methyl 2-(((triphenylstannyl)carbonothioyl)thio)propanoate **6** (1.88 g, 74%). Pink solid, mp 68–70 °C (decomposition). ^{1}H NMR (300.13 MHz, toluene-d_8, 298 K): 1.26 (m, $^{3}J_{H,H}$ = 7.1 Hz, $^{5}J_{Sn,H}$ = 3.8 Hz, 3H; $CH(C\underline{H}_3)CO_2CH_3$), 3.19 (s, 3H; $CO_2C\underline{H}_3$), 5.29 (m, $^{3}J_{H,H}$ = 7.3 Hz, $^{4}J_{Sn,H}$ = 5.9 Hz, 1H; $C\underline{H}(CH_3)CO_2CH_3$), 7.12–7.17 (m, 9H; 3-H, 4-H, $(C_6\underline{H}_5)_3Sn$), 7.54–7.78 (m, $^{3}J_{Sn,H}$ = 52.5 Hz, 6H; 2-H, $(C_6\underline{H}_5)_3Sn$); $^{13}C\{^{1}H\}$ NMR (75.47 MHz, toluene-d_8, 298 K): 16.0 (s; $CH(\underline{C}H_3)CO_2CH_3$), 43.9 (pt, $^{3}J_{Sn,C}$ = 13.2 Hz; $\underline{C}H(CH_3)CO_2CH_3$), 52.0 (s; $CH(CH_3)CO_2\underline{C}H_3$), 129.2 (pt, $^{2}J_{Sn,C}$ = 55.0 Hz; 2-C, $(\underline{C}_6H_5)_3Sn$), 129.9 (pt, $^{4}J_{Sn,C}$ = 12.2 Hz; 4-C, $(\underline{C}_6H_5)_3Sn$), 137.4 (pt, $^{3}J_{Sn,C}$ = 39.5 Hz; 3-C, $(\underline{C}_6H_5)_3Sn$), 137.6 (pt, $^{1}J_{Sn,C}$ = 541 Hz; 1-C, $(\underline{C}_6H_5)_3Sn$), 170.7 (s; $\underline{C}O_2CH_3$), 263.3 (s; $\underline{C}S_2$); $^{119}Sn\{^{1}H\}$ NMR (98.20 MHz, toluene-d_8, 298 K): −186.6. IR: 1743.4 (C=O), 1046.4 (C=S). HRMS (CI, CH_4, *m/z* of $[MH^+]$): found — 511.0178, calculated for $C_{23}H_{23}O_2S_2Sn$ — 511.0157.

Benzyl tri-p-tolylstannanecarbodithioate **7** (1.58 g, 57%). Violet crystals, m.p.: 77–79 °C. ^{1}H NMR (300.13 MHz, toluene-d_8, 298 K): 2.09 (s, 9H; $(C\underline{H}_3C_6H_4)_3Sn$), 4.46 (pt, $^{4}J_{Sn,H}$ = 4.3 Hz, 2H; $C\underline{H}_2C_6H_5$), 6.91–6.96 (m, 5H; $CH_2C_6\underline{H}_5$), 7.02 (d, $^{3}J_{H,H}$ = 7.3 Hz, 6H, 3-H, $(CH_3C_6\underline{H}_4)_3Sn$), 7.69 (m, $^{3}J_{Sn,H}$ = 43.4 Hz, $^{3}J_{H,H}$ = 7.9 Hz, 6H; 2-H, $(CH_3C_6\underline{H}_4)_3Sn$); $^{13}C\{^{1}H\}$ NMR (75.47 MHz, toluene-d_8, 298 K): 21.4 (pt, $^{5}J_{Sn,C}$ = 6.1 Hz; $(\underline{C}H_3C_6H_4)_3Sn$), 38.9 (pt, $^{3}J_{Sn,C}$ = 12.2 Hz; $\underline{C}H_2C_6H_5$), 127.4 (s; 4-C, $CH_2\underline{C}_6H_5$), 128.7 (s; 2-C, $CH_2\underline{C}_6H_5$), 129.5 (s; 3-C, $CH_2\underline{C}_6H_5$), 130.0 (pt, $^{2}J_{Sn,C}$ = 57.4 Hz; 2-C, $(CH_3\underline{C}_6H_4)_3Sn$), 134.4 (s; 1-C, $(CH_3\underline{C}_6H_4)_3Sn$), 135.9 (s; 1-C, $CH_2\underline{C}_6H_5$), 137.4 (pt, $^{3}J_{Sn,C}$ = 40.7 Hz; 3-C, $(CH_3\underline{C}_6H_4)_3Sn$), 139.5 (pt, $^{4}J_{Sn,C}$ = 12.1 Hz; 4-C, $(CH_3\underline{C}_6H_4)_3Sn$), 266.3 (s; $\underline{C}S_2$); $^{119}Sn\{^{1}H\}$ NMR (98.20 MHz, toluene-d_8, 298 K): −181.3. IR: 1040.1 (C=S). HRMS (CI, CH_4, *m/z* of $[MH^+]$): found — 559.0730, calculated for $C_{29}H_{29}S_2Sn$ — 559.0727.

1-Phenylethyl tri-p-tolylstannanecarbodithioate **8** (1.25 g, 44%). Violet crystals, m.p.: 110–112 °C. ^{1}H NMR (300.13 MHz, toluene-d_8, 298 K): 1.47 (d, $^{3}J_{H,H}$ = 7.1 Hz, 3H; $CH(C\underline{H}_3)C_6H_5$), 2.08 (s, 9H; $(C\underline{H}_3C_6H_4)_3Sn$), 5.86 (m, $^{3}J_{H,H}$ = 7.1 Hz, $^{4}J_{Sn,H}$ = 7.0 Hz, 1H; $C\underline{H}(CH_3)C_6H_5$), 6.91–6.98 (m, 5H; $CH(CH_3)C_6\underline{H}_5$), 7.01 (d, $^{3}J_{H,H}$ = 7.4 Hz, 6H; 3-H, $(CH_3C_6\underline{H}_4)_3Sn$), 7.67 (m, $^{3}J_{Sn,H}$ = 51.0 Hz, $^{3}J_{H,H}$ = 7.9 Hz, 6H; 2-H, $(CH_3C_6\underline{H}_4)_3Sn$); $^{13}C\{^{1}H\}$ NMR (75.47 MHz, toluene-d_8, 298 K): 20.1 (s; $CH(\underline{C}H_3)C_6H_5$), 21.4 (pt, $^{5}J_{Sn,C}$ = 6.0 Hz; $(\underline{C}H_3C_6H_4)_3Sn$), 46.3 (pt, $^{3}J_{Sn,C}$ = 13.2 Hz; $\underline{C}H(CH_3)C_6H_5$), 127.5 (s; 4-C, $CH(CH_3)\underline{C}_6H_5$), 128.1 (s; 2-C, $CH(CH_3)\underline{C}_6H_5$), 128.8 (s; 3-C, $CH(CH_3)\underline{C}_6H_5$), 130.0 (pt, $^{2}J_{Sn,C}$ = 56.1 Hz; 2-C, $(CH_3\underline{C}_6H_4)_3Sn$), 134.5 (s; 1-C, $(CH_3\underline{C}_6H_4)_3Sn$), 137.4 (pt, $^{3}J_{Sn,C}$ = 40.3 Hz; 3-C, $(CH_3\underline{C}_6H_4)_3Sn$), 139.4 (pt, $^{4}J_{Sn,C}$ = 12.3 Hz; 4-C, $(CH_3\underline{C}_6H_4)_3Sn$), 141.4 (s; 1-C, $CH(CH_3)\underline{C}_6H_5$), 265.5 (s; $\underline{C}S_2$); $^{119}Sn\{^{1}H\}$ NMR (98.20 MHz, toluene-d_8, 298 K): −182.9. IR: 1044.1 (C=S). HRMS (CI, CH_4, *m/z* of $[MH^+]$): found — 571.0887, calculated for $C_{30}H_{31}S_2Sn$ — 571.0885.

Methyl triphenylstannanecarbodithioate **9** (1.85 g, 84%). Pink crystals, m.p.: 127-129 °C (lit. 128-129 °C[30]). ^{1}H NMR (300.13 MHz, $CDCl_3$, 298 K): 2.77 (pt, $^{4}J_{Sn,H}$ = 2.4 Hz, 3H; $C\underline{H}_3$), 7.38–7.52 (m, 9H; 3-H, 4-H, $(C_6\underline{H}_5)_3Sn$), 7.58–7.82 (m, $^{3}J_{Sn,H}$ = 51.8 Hz, 6H; 2-H, $(C_6\underline{H}_5)_3Sn$); $^{13}C\{^{1}H\}$ NMR (75.47 MHz, $CDCl_3$, 298 K): 18.6 (pt, $^{3}J_{Sn,C}$ = 13.7 Hz; $\underline{C}H_3$), 128.9 (pt, $^{2}J_{Sn,C}$ = 55.4 Hz; 2-C, $(\underline{C}_6H_5)_3Sn$), 129.8 (pt, $^{4}J_{Sn,C}$ = 12.1 Hz; 4-C, $(\underline{C}_6H_5)_3Sn$), 137.2 (pt, $^{3}J_{Sn,C}$ = 38.5 Hz; 3-C, $(\underline{C}_6H_5)_3Sn$), 137.6 (pt, $^{1}J_{Sn,C}$ = 548.9 Hz; 1-C, $(\underline{C}_6H_5)_3Sn$), 266.6 (s; $\underline{C}S_2$); $^{119}Sn\{^{1}H\}$ NMR (98.20 MHz, $CDCl_3$, 298 K): −192.4. IR: 1045.1 (C=S). HRMS (CI, CH_4, *m/z* of $[MH^+]$): found — 442.9872, calculated for $C_{20}H_{19}S_2Sn$ — 442.9872.

Crystallographic data collection and structure determination: Single crystals of compounds **1**-**5**, **7**-**9** were selected for X-ray diffraction studies and were mounted on a microloop (MiTegen) at low temperature (193K). X-ray diffraction intensity data were measured on a Bruker-AXS SMART APEX II (**1**-**4**, **8**), Bruker-AXS Kappa APEX II Quazar (**5**, **7**) diffractometers, equipped with a 30W air-cooled microfocus source, or on a Bruker-AXS D8-Venture equipped with a CMOS Area detector (**9**) by using $Mo_{K\alpha}$ radiation (λ = 0.71073 Å). Phi- and omega- scans were used. The data were integrated with SAINT, and an empirical absorption correction with SADABS was applied.[65] The structures were solved by direct methods (SHELXS-97) and refined using the least-squares method on F^2.[66] Mercury[67] was used was used for molecular graphics. All non-H atoms were refined with anisotropic displacement parameters. The Hydrogen atoms were refined isotropically at calculated positions using a riding model. CCDC 1546707 (**1**), CCDC 1546708 (**2**), CCDC 1546709 (**3**), CCDC 1546710 (**4**), CCDC 1546711 (**5**), CCDC 1546712 (**7**), CCDC 1546713 (**8**) and CCDC1557159 (**9**) contain the supplementary crystallographic data for this paper. These data can be obtained free of charge from The Cambridge Crystallographic Data Centre.[52]

General polymerization procedure under common conditions: A solutions (5 mL) that contained the monomers, Sn-RAFT **1**-**4**,**7**,**8**, AIBN, and 1,4-dioxane in the following concentrations: $[BA]_0$=5.10 mol L^{-1}, $[St]_0$=6.00 mol L^{-1}, $[RAFT]_0$=30.0 mmol L^{-1}, $[AIBN]_0$=6.0 mmol L^{-1} were prepared in 15 mL vials, sealed with rubber septa, degassed by bubbling argon for 30 min and heated at 60 °C in a thermostated heating block. Aliquots of the reaction mixture (100 µL) were taken at given intervals, diluted with $CDCl_3$ and analyzed with ^{1}H NMR. Then the excess amount of monomer and solvent were removed by evaporation at ambient temperature under vacuum and the residues were analyzed by using SEC.

General polymerization procedure in NMR tubes: A solutions (5 mL) that contained the monomers, Sn-RAFT **4**, AIBN, and 1,4-dioxane in the following concentrations: $[BA]_0$=4.94 mol L^{-1}, $[St]_0$=5.59 mol L^{-1}, $[RAFT]_0$=93.0 mmol L^{-1}, $[AIBN]_0$=9.0 mmol L^{-1} were prepared in 15 mL Schlenk tube with PTFE needle valve and degassed by three freeze-pump-thaw cycles. Then solutions were transferred into 6 NMR tubes in the glovebox under argon atmosphere and sealed with rubber septa. Tubes were heated at 60 °C in a thermostated heating block for the requisite times, frozen in liquid nitrogen and analyzed with NMR. Then the excess amount of monomer and solvent were removed by evaporation at ambient temperature under vacuum and the residues were analyzed by using SEC.

Acknowledgements

The MESR (Ministère de l'Enseignement Supérieur et de la Recherche), the "Groupement Franco-Ukrainien en Chimie Moléculaire" GDRI and the Embassy of France in Kiev are gratefully acknowledged for financial support. The authors thank Dr. Simon Harrisson for fruitful discussions and his kind help for data treatment for the calculation of chain transfer constants, Caroline Toppan for her support during NMR measurements, Dr. Sonia Ladeira for her help during X-ray diffraction measurements

and Stanislava Mikhieieva for her help with graphical abstract design.

Keywords: RAFT polymerization • polymer • organotin • heteronuclear NMR • X-ray structure

[1] G. Moad, E. Rizzardo, S. H. Thang, *Aust. J. Chem.* **2012**, *65*, 985–1076.
[2] J. Krstina, C. L. Moad, G. Moad, E. Rizzardo, C. T. Berge, M. Fryd, *Macromol. Symp.* **1996**, *111*, 13–23.
[3] J. Chiefari, Y. K. B. Chong, F. Ercole, J. Krstina, J. Jeffery, T. P. T. Le, R. T. A. Mayadunne, G. F. Meijs, C. L. Moad, G. Moad, E. Rizzardo, S. H. Thang, *Macromolecules* **1998**, *31*, 5559–5562.
[4] T. P. Le, G. Moad, E. Rizzardo, S. H. Thang, *Polymerization with Living Characteristics*, **1998**, WO 1998001478 A1.
[5] P. Corpart, D. Charmot, T. Biadatti, S. Zard, D. Michelet, *Method for Block Polymer Synthesis by Controlled Radical Polymerisation*, **1998**, WO 1998058974 A1.
[6] D. J. Keddie, G. Moad, E. Rizzardo, S. H. Thang, *Macromolecules* **2012**, *45*, 5321–5342.
[7] G. Gody, T. Maschmeyer, P. B. Zetterlund, S. Perrier, *Macromolecules* **2014**, *47*, 3451–3460.
[8] S. Sinnwell, A. J. Inglis, T. P. Davis, M. H. Stenzel, C. Barner-Kowollik, *Chem. Commun.* **2008**, *49*, 2052–2054.
[9] M. Destarac, C. Kalai, A. Wilczewska, L. Petit, E. Van Gramberen, S. Z. Zard in *Controlled/Living Radical Polymerization* (Ed.: Krzysztof Matyjaszewski), American Chemical Society, **2006**, pp. 564–577.
[10] P. J. Roth, C. Boyer, A. B. Lowe, T. P. Davis, *Macromol. Rapid Commun.* **2011**, *32*, 1123–1143.
[11] Y. Wu, Y. Zhou, J. Zhu, W. Zhang, X. Pan, Z. Zhang, X. Zhu, *Polym. Chem.* **2014**, *5*, 5546–5550.
[12] A. B. Lowe, *Polym. Chem.* **2014**, *5*, 4820–4870.
[13] H. Willcock, R. K. O'Reilly, *Polym. Chem.* **2010**, *1*, 149–157.
[14] M. A. Harvison, P. J. Roth, T. P. Davis, A. B. Lowe, *Aust. J. Chem.* **2011**, *64*, 992–1006.
[15] G. Moad, E. Rizzardo, S. H. Thang, *Polym. Int.* **2011**, *60*, 9–25.
[16] M. Destarac, *Polym. Rev.* **2011**, *51*, 163–187.
[17] A. Theis, M. H. Stenzel, T. P. Davis, M. L. Coote, C. Barner-Kowollik, *Aust. J. Chem.* **2005**, *58*, 437–441.
[18] M. Laus, R. Papa, K. Sparnacci, A. Alberti, M. Benaglia, D. Macciantelli, *Macromolecules* **2001**, *34*, 7269–7275.
[19] R. Geagea, S. Ladeira, S. Mazières, M. Destarac, *Chem. Eur. J.* **2011**, *17*, 3718–3725.
[20] S. Mazières, I. Kulai, R. Geagea, S. Ladeira, M. Destarac, *Chem. Eur. J.* **2015**, *21*, 1726–1734.
[21] D. Matioszek, O. Brusylovets, D. James Wilson, S. Mazières, M. Destarac, *J. Polym. Sci. Part A Polym. Chem.* **2013**, *51*, 4361–4368.
[22] S. Demirci, S. Kinali-Demirci, T. Caykara, *Polymer* **2013**, *54*, 5345–5350.
[23] J. Zeng, Z. Zhang, J. Zhu, N. Zhou, Z. Cheng, X. Zhu, *J. Polym. Sci. Part A Polym. Chem.* **2013**, *51*, 2606–2613.
[24] M. Päch, D. Zehm, M. Lange, I. Dambowsky, J. Weiss, A. Laschewsky, *J. Am. Chem. Soc.* **2010**, *132*, 8757–8765.
[25] I. Kulai, O. Brusylovets, Z. Voitenko, S. Harrisson, S. Mazières, M. Destarac, *ACS Macro Lett.* **2015**, *4*, 809–813.
[26] B. Klumperman, J. B. McLeary, E. T. A. van den Dungen, G. Pound, *Macromol. Symp.* **2007**, *248*, 141–149.
[27] P. Lacroix-Desmazes, B. Améduri, B. Boutevin, Collect. Czechoslov. *Chem. Commun.* **2002**, *67*, 1383–1415.
[28] P.-R. Bolz, U. Kunze, W. Winter, *Angew. Chemie Int. Ed.* **1980**, *19*, 220–221.
[29] T. Hättich, U. Kunze, *Angew. Chemie Int. Ed.* **1982**, *21*, 364–365.
[30] U. Kunze, P. Bolz, W. Winter, *Chem. Ber.* **1981**, *114*, 2744–2753.
[31] S. W. Carr, R. Colton, D. Dakternieks, B. F. Hoskins, R. J. Steen, *Inorg. Chem.* **1983**, *22*, 3700–3706.
[32] B. Mathiasch, U. Kunze, *Inorganica Chim. Acta* **1983**, *75*, 209–213.
[33] U. Kunze, P.-R. Bolz, *Zeitschrift für Anorg. und Allg. Chemie* **1983**, *498*, 41–49.
[34] U. Kunze, P.-R. Bolz, *Zeitschrift für Anorg. und Allg. Chemie* **1983**, *498*, 50–56.
[35] U. Kunze, R. Tischer, *Chem. Ber.* **1987**, *120*, 1099–1104.
[36] W. Hiller, U. Kunze, R. Tischer, *Inorganica Chim. Acta* **1987**, *133*, 51–55.
[37] W. Thiel, R. Mayer, *J. für Prakt. Chemie* **1989**, *331*, 243–262.
[38] I. Kulai, O. Brusylovets, N. Saffon, Z. Voitenko, S. Mazières, M. Destarac, *Fr.-Ukr. J. Chem.* **2015**, *3*, 53–59.
[39] C. C. Cummins, C. Huang, T. J. Miller, M. W. Reintinger, J. M. Stauber, I. Tannou, D. Tofan, A. Toubaei, A. Velian, G. Wu, *Inorg. Chem.* **2014**, *53*, 3678–3687.
[40] K. Kpegba, P. Metzner, *Synthesis* **1989**, *1989*, 137–139.
[41] M. Zamfir, C. S. Patrickios, F. Montagne, C. Abetz, V. Abetz, L. Oss-Ronen, Y. Talmon, *J. Polym. Sci. Part A Polym. Chem.* **2012**, *50*, 1636–1644.
[42] N. Azizi, F. Aryanasab, M. R. Saidi, *Org. Lett.* **2006**, *8*, 5275–5277.
[43] D. Hua, R. Bai, W. Lu, C. Pan, *J. Polym. Sci. Part A Polym. Chem.* **2004**, *42*, 5670–5677.
[44] T. Congdon, R. Notman, M. I. Gibson, *Biomacromolecules* **2013**, *14*, 1578–1586.
[45] J. Chiefari, R. T. A. Mayadunne, C. L. Moad, G. Moad, E. Rizzardo, A. Postma, S. H. Thang, *Macromolecules* **2003**, *36*, 2273–2283.
[46] D. Mozhdehi, J. A. Neal, S. C. Grindy, Y. Cordeau, S. Ayala, N. Holten-Andersen, Z. Guan, *Macromolecules* **2016**, *49*, 6310–6321.
[47] E. Bicciocchi, Y. K. Chong, L. Giorgini, G. Moad, E. Rizzardo, S. H. Thang, *Macromol. Chem. Phys.* **2010**, *211*, 529–538.
[48] L. Nebhani, S. Sinnwell, C. Y. Lin, M. L. Coote, M. H. Stenzel, C. Barner-Kowollik, *J. Polym. Sci. Part A Polym. Chem.* **2009**, *47*, 6053–6071.
[49] A. Favier, M. T. Charreyre, *Macromol. Rapid Commun.* **2006**, *27*, 653–692.
[50] Y. K. Chong, J. Krstina, T. P. T. Le, G. Moad, A. Postma, E. Rizzardo, S. H. Thang, *Macromolecules* **2003**, *36*, 2256–2272.
[51] D. J. Keddie, *Chem. Soc. Rev.* **2014**, *43*, 496–505.
[52] F. H. Allen, *Acta Crystallogr. Sect. B Struct. Sci.* **2002**, *58*, 380–388.
[53] P. C. Chieh, J. Trotter, *J. Chem. Soc. A Inorganic, Phys. Theor.* **1970**, 911–914.
[54] J. P. García-Merinos, H. López-Ruiz, Y. López, S. Rojas-Lima, *Acta Crystallogr. Sect. E Struct. Reports Online* **2014**, *70*, o584–o585.
[55] S. Xiao, R. Gu, P. A. Charpentier, *Acta Crystallogr. Sect. E Struct. Reports Online* **2011**, *67*, o1442–o1442.
[56] X. Lin, S. Zhang, Z. Liu, H. Wang, R. Cao, *Chem. J. Chinese Univ.* **1985**, *6*, 823–826.
[57] R. Moreno-Fuquen, C. Grande, F. Zuluaga, J. Ellena, C. A. De Simone, *Acta Crystallogr. Sect. E Struct. Reports Online* **2010**, *66*, o2614–o2614.
[58] D. Abe, Y. Sasanuma, *Acta Crystallogr. Sect. E Struct. Reports Online* **2013**, *69*, o1636–o1636.
[59] M. Kannan, V. Ramkumar, R. Dhamodharan, *Acta Crystallogr. Sect. E Struct. Reports Online* **2011**, *67*, o3352–o3352.
[60] R. Moreno-Fuquen, C. Grande, R. C. Advincula, J. C. Tenorio, J. Ellena, *Acta Crystallogr. Sect. E Struct. Reports Online* **2013**, *69*, o774–o774.
[61] J. Lad, S. Harrisson, G. Mantovani, D. M. Haddleton, Dalt. Trans. 2003, 4175–4180.
[62] T. Gruendling, T. Junkers, M. Guilhaus, C. Barner-Kowollik, *Macromol. Chem. Phys.* **2010**, *211*, 520–528.
[63] K. A. Kozeschkow, M. M. Nadj, A. P. Alexandrow, *Berichte der Dtsch. Chem. Gesellschaft* **1934**, *67*, 1348–1349.
[64] P. Preiffer, *Zeitschrift für Anorg. Chemie* **1910**, *68*, 102–122.
[65] SADABS, Program for data correction.
[66] G. M. Sheldrick, *Acta Crystallogr. Sect. A Found. Crystallogr.* **2008**, *64*, 112–122.
[67] C. F. Macrae, I. J. Bruno, J. A. Chisholm, P. R. Edgington, P. McCabe, E. Pidcock, L. Rodriguez-Monge, R. Taylor, J. van de Streek, P. A. Wood, *J. Appl. Crystallogr.* **2008**, *41*, 466–470.

10.1002/chem.201703412

WILEY-VCH

FULL PAPER

A series of triarylstannane-carbodithioates was synthesized. Introduction of bulky and strongly electron-positive tin makes them highly reactive reversible addition-fragmentation chain transfer agents in the free-radical polymerization of styrene and *n*-butyl acrylate. ^{119}Sn NMR allows the monitoring of their transformations during polymerization.

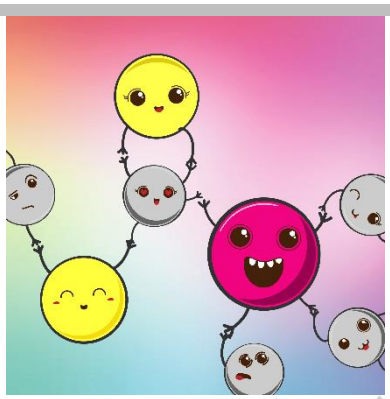

Ihor Kulai, Nathalie Saffon-Merceron, Zoia Voitenko, Stéphane Mazières and Mathias Destarac

Page No. – Page No.

Alkyl Triarylstannanecarbodithioates: Synthesis, Crystal Structures and Efficiency in RAFT Polymerization